Effects of delayed recovery and nonuniform transmission on the spreading of diseases in complex networks

C.Y. Xia[a,b], Z. Wang[b,c,d], J. Sanz[b,e], S. Meloni[b] and Y. Moreno[b,e]

[a] *Key Laboratory of Computer Vision and System (Ministry of Education) and Tianjin Key Laboratory of Intelligence Computing and Novel Software Technology, Tianjin University of Technology, Tianjin 300384, P.R.China*

[b] *Institute for Biocomputation and Physics of Complex Systems (BIFI), University of Zaragoza, 50018 Zaragoza, Spain*

[c] *Department of Physics, Hong Kong Baptist University, Kowloon Tong, Hong Kong*

[d] *Center for Nonlinear Studies and the Beijing-Hong Kong-Singapore Joint Center for Nonlinear and Complex Systems (Hong Kong) Baptist University, Kowloon Tong, Hong Kong.*

[e] *Department of Theoretical Physics, University of Zaragoza, 50009 Zaragoza, Spain*

Abstract

We investigate the effects of delaying the time to recovery (delayed recovery) and of nonuniform transmission on the propagation of diseases on structured populations. Through a mean-field approximation and large-scale numerical simulations, we find that postponing the transition from the infectious to the recovered states can largely reduce the epidemic threshold, therefore promoting the outbreak of epidemics. On the other hand, if we consider nonuniform transmission among individuals, the epidemic threshold increases, thus inhibiting the spreading process. When both mechanisms are at work, the latter might prevail, hence resulting in an increase of the epidemic threshold with respect to the standard case, in which both ingredients are absent. Our findings are of interest for a better understanding of how diseases propagate on structured populations and to a further design of efficient immunization strategies.

Keywords: Disease Spreading, Complex Networks, SIS model, Heterogeneous Mean-Field approach.

1. Introduction

Infectious diseases have been a great threat to human being since long time ago [1]. Especially in the recent years, some emerging infectious diseases, such as severe acute respiratory syndrome(SARS) [2], avian influenza [3, 4], and swine influenza [5], have resulted in huge life and economical losses. Thus, analyzing and understanding the propagation of infectious diseases is of great significance to efficiently control potentially devastating epidemic outbreaks as well as to deploy tailored immunization strategies. Traditionally, there are two typical epidemic models: the Susceptible-Infected-Susceptible (SIS) and the Susceptible-Infected-Removed (SIR) models. Both kinds of models have been intensively studied during the last years, adding to the traditional well-mixed hypothesis usually invoked by the models [6] an ever increasing dose of realism.

As a matter of fact, real systems are neither regular (and/or well-mixed) nor random, but their topology is usually different to these limits [7, 8]. Actually, the more abundant are those called scale-free (SF) networks, in which the probability $P(k)$ that an individual has k neighbors is a power-law distribution [8, 9]. Today, the modeling of infectious diseases and their prevention and control has become an interdisciplinary issue which has attracted the attention of scientists from Epidemiology, Biology, Mathematics, Physics and Computational Sciences [10–13]. In particular, Pastor-Satorras and Vespignani [14, 15] showed that the epidemic threshold λ_c in a SIS model is absent for SF networks in the thermodynamic limit, that is, the threshold λ_c approaches zero and even a vanishingly small infection rate can produce an outbreak. Similar conclusions were also found for the SIR model on SF networks by Moreno et al [16]. These alarming results have inspired a great number of related works, and most results point out that the topology of interactions dominates the spreading dynamics in complex networks [17–29].

Other works have also explored the effects of different infection mechanisms. For instance, in Ref.[30], the authors proposed a kind of connectivity-dependent infection scheme, which can yield threshold effects even in scale-free networks where they would otherwise be unexpected. Additional ingredients include saturation effects [31], constant infectivity [32], nonuniform transmission [33], finite populations [34], traffic-driven mechanisms [35], and piece-wise infection probability [36], which have been integrated into the SIS or SIR models.

On the other hand, there are other realistic elements that have been par-

tially addressed in recent studies. For instance, the issue of delayed recovery can be thought off as the time elapsed since an individual becomes infected and the moment he/she starts the treatment that could lead to recovery [37, 38]. This is especially relevant when studying spreading dynamics of diseases for which spontaneous recovery not due to medical treatment is unlikely. In what follows, we study the effects of such delayed recovery on the epidemic thresholds of a SIS dynamics that takes place on top of homogeneous and heterogeneous networks. Moreover, we also consider the case of nonuniform transmission (i.e., the fact that the spreading capabilities of an individual depend on his/her number of contacts) and the situation in which both mechanisms are concurrently active. To this end, we make use of the heterogeneous mean-field theory and performs large-scale numerical simulations, which we show are in agreement with the analytical predictions.

The rest of this paper is organized as follows. Section 2 describes in detail our model. In Section 3, the mean-field theory is used to derive the epidemic thresholds for homogeneous and heterogeneous networks. Large-scale numerical Monte Carlo simulations are also carried out to validate the mean-field approximation in Section 3. Finally, in Section 4, we round off the paper by presenting our concluding remarks.

2. The Model

In the standard SIS model, individuals are divided into two categories: Susceptible (S) and Infected (I). Susceptible individuals are healthy ones which can be infected with the probability β through contacts with infectious subjects. Infective individuals on its turn are recovered with the probability γ, which we henceforth set to 1. Hence, individuals go through the cycle $S \longrightarrow I \longrightarrow S$, their dynamics being described by,

$$\begin{cases} \frac{ds(t)}{dt} = -\gamma\rho(t) + \beta s(t)\rho(t) \\ \frac{d\rho(t)}{dt} = \gamma\rho(t) - \beta s(t)\rho(t). \end{cases} \tag{1}$$

where $s(t)$ and $\rho(t)$ stand for the fraction of susceptible and infective individuals. Generally, we neglect the details of disease infection and fix the size of the total population, and thus $s(t)$ and $\rho(t)$ need to satisfy the normalization condition: $s(t) + \rho(t) = 1$.

In our modified SIS model with nonuniform spreading (transmission) probabilities and delayed recovery, we still assume that individuals can be susceptible or infectious. However, we introduce two new ingredients:

- If an individual is infected by his/her infected neighbors at any time step t, it will be infectious during a time window $T+1$. Once this time has elapsed, the infective agent goes back to the susceptible state, S, with probability $\gamma = 1$, which can be assumed without loss of generality.

- At each time step t, infected individuals spread the disease to susceptible nodes with a probability that depends on the number of connections it has. Therefore, we assume that the effective spreading rate $\lambda = \beta/\gamma$ is a degree-dependent function $\lambda(k) = \frac{\lambda_0 k^\alpha}{k}$ (i.e., so-called nonuniform transmission).

The flow diagram of the disease spreading process for our modified model can be seen in Fig. 1, in which $I_0, I_1, ..., I_T$ denote the infective individuals at different stages and S represents the susceptible agents.

3. Epidemic Thresholds

In this section, we investigate the critical thresholds of the model in both homogeneous and heterogeneous networks.

3.1. Homogeneous topology

In homogeneous networks, the degree distribution is highly peaked around the average degree of the graph and the probability of finding a node with degree larger than the average degree $\langle k \rangle$ decays exponentially fast as we move away from the peak. Making use of the mean-field approximation [14, 15], we can assume the connectivity of each node to be constant and equal to $\langle k \rangle$. In this case, also $\lambda(k)$ becomes constant for all the nodes and reads as $\lambda(k) = \lambda' = \frac{\lambda_0 \langle k \rangle^\alpha}{\langle k \rangle}$. Now, we can write the dynamical equations describing the system dynamics as:

$$\begin{cases} \frac{\partial s(t)}{\partial t} = -\lambda' \langle k \rangle s(t)\rho(t) + \rho_T(t) \\ \frac{\partial \rho_0(t)}{\partial t} = -\rho_0(t) + \lambda' \langle k \rangle s(t)\rho(t) \\ \frac{\partial \rho_1(t)}{\partial t} = -\rho_1(t) + \rho_0(t) \\ ... \\ \frac{\partial \rho_T(t)}{\partial t} = -\rho_T(t) + \rho_{T-1}(t) \end{cases} \tag{2}$$

where $s(t)$ is the fraction of susceptible individuals, $\rho_0(t)$, ...,$\rho_T(t)$ denote the fraction of individuals in the states I_0, ..., I_T, respectively, and $\rho(t) =$

$\sum_0^T \rho_j(t)$. The first equation in Eqs.(2) represents the time evolution of susceptible individuals while the rest of equations stand for the evolution of each of the T stages through which infected individuals pass until final recovery. In the first equation the negative term accounts for the new contagions and a positive term stands for recovered infected individuals. In the rest of the eqs. each negative term represents nodes passaging to the next stage of the recovery time while the positive one includes the passage from the previous stage to the present. If we insert the normalization condition $s(t) + \rho(t) = 1$ into Eqs.(2), we get

$$\frac{\partial \rho_0(t)}{\partial t} = -\rho_0(t) + \lambda' \langle k \rangle [1 - \rho(t)]\rho(t). \tag{3}$$

When $t \longrightarrow \infty$, the system reaches a stationary state in which $\frac{\partial \rho_\tau(t)}{\partial t} = 0$ for $\tau = 0, 1, ..., T$, and hence,

$$\rho_0 = \rho_1 = ... = \rho_T, \tag{4}$$

where ρ_0, ρ_1, ..., ρ_T and ρ respectively denote the steady state values of $\rho_0(t)$, $\rho_1(t)$, ..., $\rho_T(t)$ and $\rho_(t)$. Finally, we have,

$$\rho_0 = \rho_1 = ... = \rho_T = \frac{\rho}{T+1}. \tag{5}$$

Combining Eq.(2) and Eq.(5), one obtains

$$-\frac{\rho}{T+1} + \lambda' \langle k \rangle (1 - \rho)\rho = 0. \tag{6}$$

Obviously, $\rho = 0$ is a trivial solution of Eq.(6), which corresponds to the disease-free state. To obtain a nontrivial solution $0 < \rho < 1$ which would represent an endemic state, the following condition must be fulfilled,

$$\frac{d}{d\rho}[\lambda' \langle k \rangle (T+1)(\rho - \rho^2)]|_{\rho=0} > 1. \tag{7}$$

That is,

$$\lambda' \langle k \rangle (T+1) > 1, \tag{8}$$

and thus, the critical threshold can be written as:

$$\lambda_0^c = \frac{1}{(T+1)\langle k \rangle^\alpha}. \tag{9}$$

Although Eq.(9) represents the general values of the epidemic threshold, some particular cases are worth of further discussion:

- When the recovery delay is absent (i.e., $T = 0$), the critical threshold is governed by the nonuniform transmission $\lambda_0^c = \frac{1}{\langle k \rangle^\alpha}$. In particular, $\alpha = 1$ stands for the standard case where the critical spreading rate is equal to the inverse of the average degree of the network, for which we recover the classical result $\lambda_0^c = \frac{1}{\langle k \rangle}$ [15].

- when $\alpha = 0$, if we introduce a rescaling factor A at the pre-factor of $\lambda(k)$ we get $\lambda(k) = A\lambda_o \langle k \rangle^{-1}$. In this case, the critical threshold reads as $\lambda_o^c = \frac{1}{T+1} \cdot \frac{1}{A}$, and therefore the threshold is independent of the network topology. This rescaling leads, in the particular case of $T = 0$, to $\lambda_o^c = \frac{1}{A}$[32].

3.2. Heterogeneous topology

For many natural, social and engineering systems, the degree distribution is highly skewed, that is, the topology is very heterogeneous and the average degree is not anymore a good proxy for the degree of each individual. In this case, nonuniform transmission effects are expected to be much more relevant in terms of their influence on the spreading dynamics, as the degree dependence of the spreading rate $\lambda(k) = \frac{\lambda_0 k^\alpha}{k}$ is explicitly incorporated. Hence, we should write differential equations for each class of degree k, which read as

$$\begin{cases} \frac{\partial s_k(t)}{\partial t} = -k s_k(t)\Theta_k(t) + \rho_{k,T}(t) \\ \frac{\partial \rho_{k,0}(t)}{\partial t} = -\rho_{k,0}(t) + k s_k(t)\Theta_k(t) \\ \frac{\partial \rho_{k,1}(t)}{\partial t} = -\rho_{k,1}(t) + \rho_{k,0}(t) \\ \ldots \\ \frac{\partial \rho_{k,T}(t)}{\partial t} = -\rho_{k,T}(t) + \rho_{k,T-1}(t) \end{cases} \tag{10}$$

where $\rho_{k,T}(t)$ denotes the fraction of individuals with degree k in state I_T at time t, and $\Theta_k(t)$ is the probability that a link points to an infected individual. The general expression for $\Theta_k(t)$ is,

$$\Theta_k(t) = \sum_{k'} \lambda(k) P(k'|k) \rho_{k'}(t). \tag{11}$$

where $\rho_{k'}(t)$ is the density of infected individuals with degree k' and the conditional probability $P(k'|k)$ denotes the probability that a node with degree k is connected to a node with degree k'. We assume that networks are uncorrelated, and so $\Theta_k(t) = \Theta_{k'}(t) \equiv \Theta(t)\ \forall(k, k')$, and $P(k'|k) =$

$k'P(k')/\sum_s sP(s)$, which gives:

$$\Theta(t) = \sum_{k'} \frac{\lambda(k')k'P(k')\rho_{k'}(t)}{\sum_s sP(s)} = \frac{\sum_{k'} \lambda(k')k'P(k')\rho_{k'}(t)}{\langle k \rangle}. \tag{12}$$

At the steady state, $\frac{\partial \rho_{k,\tau}(t)}{\partial t} = 0$ for $\tau = 0, 1, ..., T$, and let $\rho_k(t) = \sum_{\tau=0}^{T} \rho_{k,\tau}(t)$ be the density of infected individuals with degree k, with the steady state values of $\rho_k(t)$, $\rho_{k,0}(t)$, ..., $\rho_{k,T}(t)$ labeled as ρ_k, $\rho_{k,0}$, ..., $\rho_{k,T}$, respectively. Eq.(10) can be reduced to,

$$\begin{cases} -\rho_{k,0} + k(1-\rho_k)\Theta = 0 \\ -\rho_{k,1} + \rho_{k,0} = 0 \\ ... \\ -\rho_{k,T} + \rho_{k,T-1} = 0 \end{cases} \tag{13}$$

Inserting $\rho_k = \sum_{\tau=0}^{T} \rho_{k,\tau}$ into Eq.(13), we obtain,

$$\begin{cases} \rho_{k,0} = \rho_{k,1} = ... = \rho_{k,T} = \frac{\rho_k}{T+1} \\ \rho_k = \frac{k\Theta}{\frac{1}{T+1} + k\Theta} \end{cases} \tag{14}$$

which gives,

$$\Theta = \frac{1}{\langle k \rangle} \sum_{k'} \lambda(k')k'P(k') \frac{k'\Theta}{\frac{1}{T+1} + k'\Theta}. \tag{15}$$

$\Theta = 0$ is a trivial solution of Eq.(15) which corresponds to the absence of an outbreak. In order to have a nontrivial solution, $0 < \Theta < 1$, the following condition must be satisfied,

$$\frac{d}{d\Theta}[\frac{1}{\langle k \rangle} \sum_{k'} \lambda(k')k'P(k') \frac{k'\Theta}{\frac{1}{T+1} + k'\Theta}]|_{\Theta=0} > 1. \tag{16}$$

That is,

$$\frac{1}{\langle k \rangle} \sum_{k'} \lambda(k')k'P(k')k'(T+1) > 1. \tag{17}$$

Again, according to Eq.(17), there are different scenarios worth addressing:

- If we assume that the nonuniform transmission effect is absent and so the spreading rate is independent of the degree of the nodes (i.e. $\alpha = 1$), then $\lambda(k) = \lambda_0 k/k = \lambda_0$ and Eq.(17) reads as,

$$\lambda_o > \frac{1}{T+1} \cdot \frac{\langle k \rangle}{\langle k^2 \rangle}. \tag{18}$$

  That is, the threshold $\lambda_0^c = \frac{1}{T+1} \cdot \frac{\langle k \rangle}{\langle k^2 \rangle}$. In particular, $T = 0$ gives $\lambda_0^c = \frac{\langle k \rangle}{\langle k \rangle^2}$ which recovers the classical result [15].

- If the spreading rate is proportional to the inverse of the degree (i.e. $\alpha = 0$, maximum nonuniform transmission), we recover the expression previously obtained for the homogeneous network, i.e.,

$$\lambda_0^c = \frac{1}{(T+1)} \cdot \frac{1}{A}. \tag{19}$$

- For intermediate cases, i.e., $\lambda(k) = \lambda_0 k^\alpha/k$ with $0 < \alpha < 1$, the critical threshold reads as

$$\lambda_0^c = \frac{1}{T+1} \cdot \frac{\langle k \rangle}{\langle k^{1+\alpha} \rangle}. \tag{20}$$

  where $\alpha = 0$ and $\alpha = 1$ corresponds to two extreme cases previously analyzed.

3.3. Numerical Results

With the aim of validating the mean-field results, we next perform large scale numerical simulations on random (ER like) networks (generated using the Watts-Strogatz (WS) model with rewiring probability $p = 1$) and BA scale-free networks. All simulation results are averages over 100 independent runs and, unless otherwise stated, the size of the networks is $N = 5000$. Moreover, we set the average degree of both kinds of graphs to be $\langle k \rangle = 8$ and simulations have been done using a recovery rate $\gamma = 1$.

Figure 2 shows the steady-state density of infected individuals or prevalence $\rho(\infty)$ as a function of the effective spreading rate λ_0 in both networks. Here we do not consider any recovery delay, that is, $T = 0$. In the figure, the arrows correspond to the analytical results for the epidemic thresholds for several values of α as indicated. In most cases, the analytical predictions agree well with the results of numerical simulations. However, for $\alpha = 0$ and

$A = 3$, the theoretical results are slightly different to the numerical ones, which we think is due to finite size effects. In any case, the figure nicely shows that the critical thresholds for an outbreak to occur can be largely altered by this scheme.

On the other hand, Figure 3 illustrates the effects of the second mechanism −the delayed recovery− when it is the only ingredient at work with respect to the standard case. Again, the results from numerical simulations are in accordance with our mean-field calculations and confirm that if infected individuals remain so for longer times, the critical threshold is reduced.

Another scenario of interest corresponds to the case in which the spreading rate is inversely proportional to the degree of each individual (i.e. $\lambda = \lambda_o k^{-1}$ which means that $\alpha = 0$). As it can be shown, in this case, in what regards the epidemic thresholds whether the network is homogeneous or heterogeneous is completely irrelevant, provided that both kinds of graphs have the same $\langle k \rangle$. Figure 4 shows the numerical results, which confirm that the underlying networks do not determine the epidemic thresholds. Actually, they are the same in both panels for all values of T simulated.

Figure 5 describes what happens when both mechanisms are simultaneously active. Essentially, a delay in recovery will make the epidemic threshold smaller than for the standard case and unless the dependence of the spreading rate compensates for this effect, the disease-free regime will be shortened, as it happens after our parameter election in this case.

Finally, with the aim to clarify the nature of the small discrepancies between numerical results and the analytical predictions of Eq.(20), in Fig. 6 we consider the influence of network size on the epidemic threshold. Results highlight that, as expected, the critical threshold decreases as the network size increases. Simultaneously, the mismatch between numerical and theoretical values drops, suggesting that the initial differences are due to finite size effects.

4. Conclusions and Discussions

In summary, we have studied the effects of increasing the infectious period of infected individuals that at the same time transmit the disease with a spreading rate which decreases with the number of neighbors. The latter mechanism is intended to model situations in which subjects avoid contacting all of their neighbors and therefore their contagion capabilities are reduced. The former, on the contrary, accounts for a common attitude of sick subjects,

who quite often refrain from taking a treatment from the very initial stages of the disease, thus delaying their recovery. Through a mean-field analysis and numerical simulations, we have shown that the delayed recovery reduces the epidemic threshold whereas the nonuniform spreading has the opposite effect. It is worth stressing that in our model, the delayed recovery is introduced as an independent parameter, and not through smaller values of γ, as the latter is a parameter that characterizes the disease and we are accounting for a behavioral reaction, i.e., that of postponing the treatment. When both ingredients are simultaneously present, whether or not the new effective epidemic threshold is reduced with respect to the standard case depends on their interplay: if contacts between spreaders and susceptible individuals are significantly reduced as it could be the case in a real epidemic, then the disease-free region will be larger. Otherwise, the longer permanence of infected subjects as so will not be compensate by their reduced contagion capabilities. Altogether, our results point out that in order for different countermeasures to be effective, which usually include isolation of sick individuals and therefore cutting down the number of potential susceptible-infectious contacts, other aspects as the presence of "free-riders" that delay their recovery should also be taken into account.

In addiction, our results add a further piece in our understanding of epidemic processes on large networks and pave the way to more realistic models. A step in this direction could be represented by the inclusion of delayed recovery and nonuniform transmission schemes into time-evolving spreading models [39, 40], which reproduce better real-world scenarios with respect to the use of static networks.

Acknowledgements

C.Y. Xia is partially supported by the National Natural Science Foundation of China under Grant No. 60904063, Tianjin Municipal Natural Science Foundation under Grant No. 11JCYBJC06600 and the 7th Overseas Training Project for the Young and Middle Teachers in Tianjin Municipal Universities. S.M. is supported by the Spanish Ministry of Science and Innovation (MICINN) through project FIS2009-13364-C02-01. Y. M. is supported by the Spanish MICINN through projects FIS2009-13364-C02-01 and FIS2011-25167 and by the Government of Aragón through a grant to FENOL.

References

[1] S. Eubank, H. Guclu, V.S.A. Kumar et al. Nature, 429(2004) 180.

[2] R.A.M. Fouchier, T. Kuiken, M. Schutten et al. Nature, 423(2003) 240.

[3] H.B. John, F. Jeremy, M.H. Aye et al. New J. Eng. Med., 353(2005) 1374.

[4] M. Small, D.M. Waker and C.K. Tse. Phys. Rev. Lett., 99(2007) 188702.

[5] C. Fraser, C.A. Donnelly, S. Cauchemez et al. Science, 324(2009) 1557.

[6] H.W. Hethcote. SIAM Review, 42(2000) 599.

[7] D.J. Watts and S.H. Strogatz. Nature, 393(1998) 440.

[8] A.L. Barabási and R. A1bert. Science, 286(1999) 509.

[9] S.Boccaletti, V. Latora, Y. Moreno, M. Chaverz and D.U. Hwang. Physics Reports, 424(2006) 175.

[10] M.J. Keeling and K.T.D. Eames. J. R. Soc. Interface, 2(2005) 295.

[11] R.M. May. Trends Ecol. Evol., 32(2006) 394.

[12] L.A. Meyers. Bull. Am. Math. Soc., 44(2007) 63.

[13] J. Zhou and Z.H.Liu. Front. Phys. China, 3(2008) 331.

[14] R. Pastor-Satorras and A. Vespignani. Phys. Rev. Lett., 86(2001) 3200.

[15] Pastor-Satorras R. and Vespignani A. Phys. Rev. E , 63(2001) 066117.

[16] Y. Moreno, R. Pastor-Satorras and A. Vespignani. European Physical Journal B, 26(2002) 521.

[17] M.E.J. Newman. Phys. Rev. E , 66(2002) 016128.

[18] M. Boguna, R. Pastor-Satorras and A. Vespignani. Phys. Rev. Lett., 90 (2003) 028701.

[19] M. Barthelemy, A.Barrat, R. Pastor-Satorras and A. Vespiganani. Phys. Rev. Lett., 92(2004) 178701.

[20] X.Y. Wu and Z.H. Liu. Physica A, 387(2008) 623.

[21] J. Sanz, L.M. Floria and Y. Moreno. Phys. Rev. E, 81(2010) 056108.

[22] M. Tang, Z.H. Liu and B.W. Li. EPL, 87(2009) 18005.

[23] S. Meloni, N. Perra, A. Arenas et al. Scientific Reports, 1(2011) 62.

[24] L. Wang, X. Li, Y.Q. Zhang, Y. Zhang and K. Zhang, PLoS ONE, 6(2011): e21197.

[25] H.J. Shi, Z.S. Duan and G.R. Chen. Physica A, 387(2008) 2133.

[26] S.Gómez, A. Arenas, J. Borge-Holthoefer, S. Meloni and Y. Moreno. EPL, 89(2010) 38009.

[27] C.Y. Xia, Z.X. Liu, Z.Q. Chen and Z.Z. Yuan. Prog. Nat. Sci., 17(2007) 358.

[28] C.Y. Xia, Z.X. Liu, Z.Q. Chen, S.W. Sun and Z.Z. Yuan. Prog. Nat. Sci., 18(2008) 763.

[29] C.Y. Xia, S.W. Sun, Z.X. Liu, Z.Q. Chen and Z.Z. Yuan. Int. J. Mod. Phys. B, 23(2009) 2203.

[30] R. Olinky and L. Stone. Phys. Rev. E, 70(2004) 030902.

[31] J. Joo and J.L. Lebowitz. Phys. Rev. E, 69(2004) 066105.

[32] R. Yang, B.H. Wang, Ren. J et al. Phys. Lett. A, 364(2007) 189.

[33] J.Z. Wang, Z.R. Liu and J.H. Xu. Physica A, 382(2007) 715.

[34] J. Gómez-Gardeñes, V. Latora, Y. Moreno and E. Profumo. Proc. Natl. Acad. Sci. USA, 105 (2008) 1399.

[35] S. Meloni, A. Arenas and Y. Moreno, Proc. Natl. Acad. Sci. USA, 106 (2009), 16897.

[36] X.C. Fu, M. Small, D.M. Walker et al. Phys. Rev. E, 77(2008) 036113.

[37] C.G. Li and G.R. Chen. Physica A, 343(2004) 263.

[38] X.J. Xu, H.O. Pen, X.M. Wang and Y.H. Wang. Physica A, 367(2006) 525.

[39] M.C. González and H.J. Herrmann. Physica A, 340(2004) 741.

[40] M.C. González, H.J. Herrmann and A.D. Araújo. Physica A, 356(2005) 100.

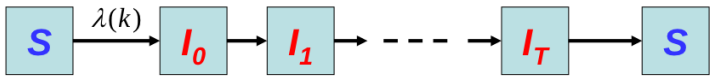

Figure 1: The figure shows the cycle of infection of a susceptible individual. We assume that after the initial infection, the newly infected node will remain infectious during a time window of $T+1$ time steps, after which the node recovers and gets back to the susceptible state.

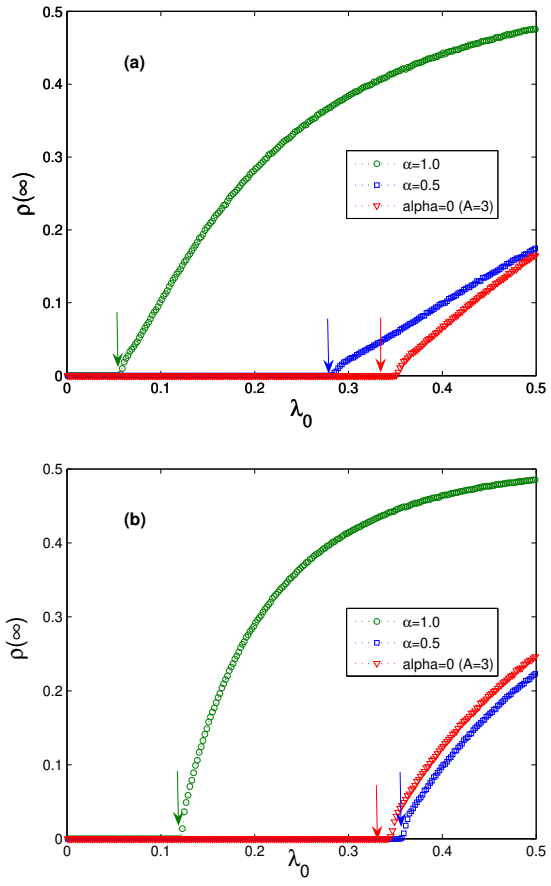

Figure 2: The effect of degree-dependent spreading rates on the propagation of diseases in complex networks. In this case, the delayed recovery mechanism is not present. (a) BA scale-free model; (b) Random WS model ($p = 1$). All data points are obtained after averaging 100 independent runs and the dashed lines are a guide to the eyes. The arrows denote the epidemic thresholds as given by the analytical results. The parameter A in these figures plays the role of an scaling factor for the critical point. When $A = 1$, the contact process is recovered for the case $\alpha = 0$ and so, the critical point is $\lambda_0^c = 1$.

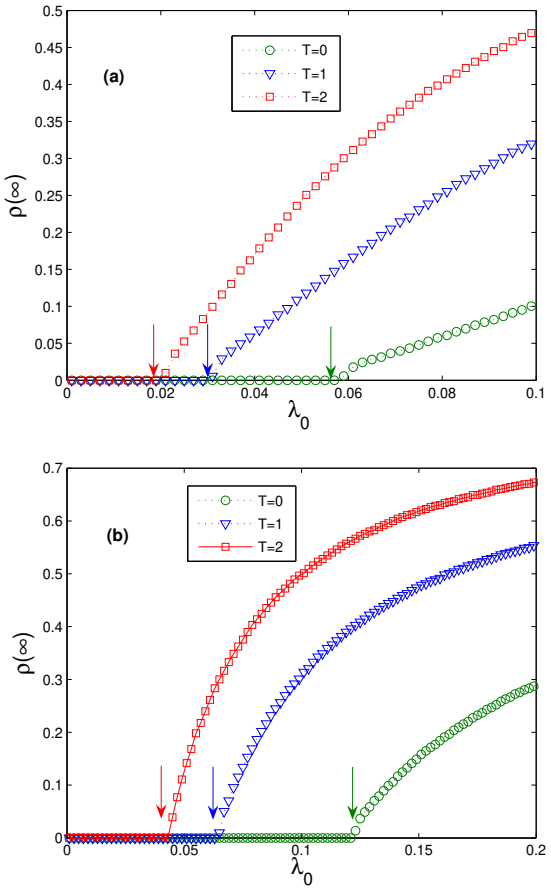

Figure 3: Effect of the delayed recovery in the absence of the degree-dependent spreading rates scenario (i.e. $\alpha = 1.0$). (a) BA scale-free model; (b) Random WS model ($p = 1$). All data points are obtained after averaging 100 independent runs and the dashed lines are a guide to the eyes. The arrows denote the epidemic thresholds as given by the analytical results.

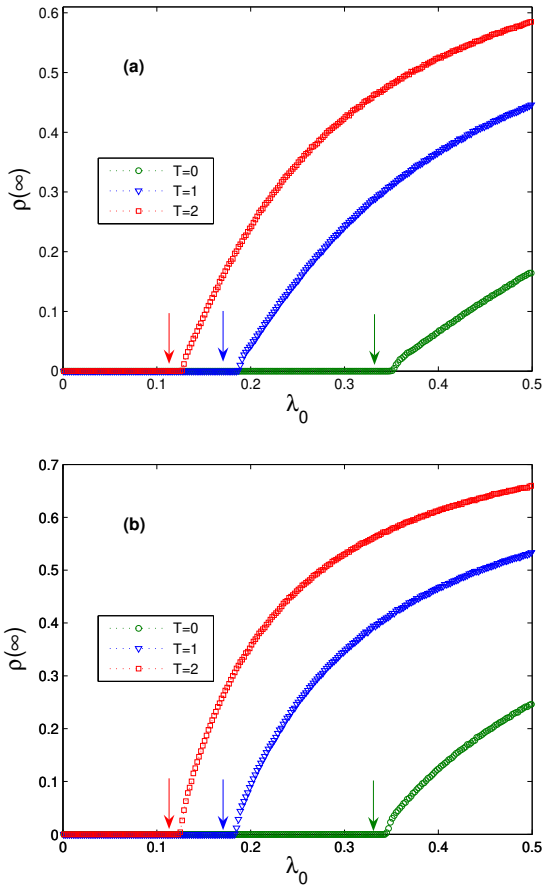

Figure 4: Same results as in Figure 3 but for $\alpha = 0$ and $A = 3$. (a) BA scale-free model; (b) Random WS model ($p = 1$). All data points are obtained after averaging 100 independent runs and the dashed lines are a guide to the eyes. The arrows denote the epidemic thresholds as given by the analytical results.

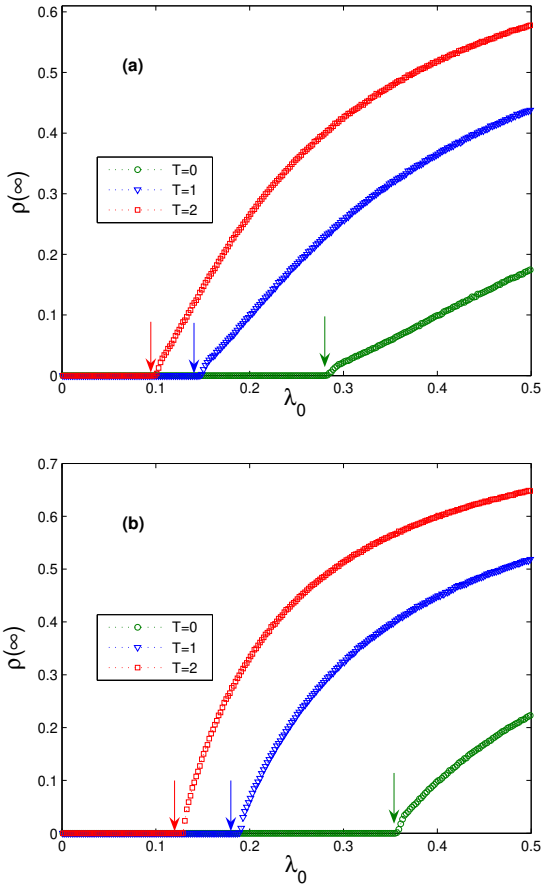

Figure 5: Numerical results when both mechanisms studied are concurrently active. (a) BA scale-free model; (b) Random WS model ($p = 1$). The value of α have been set to 0.5. Arrows identify the epidemic thresholds as given by the mean-field approach.

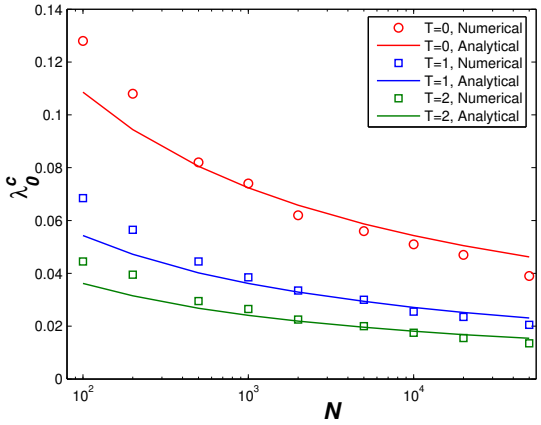

Figure 6: Comparison of critical threshold between the numerical simulations and analytical results in Eq.(20) in which α is fixed to be 1.0 and the network parameters are set to be $m = m0 = 4$ in BA model.